Chemical Engineering Journal 166 (2011) 445–453

Contents lists available at ScienceDirect

Chemical Engineering Journal

journal homepage: www.elsevier.com/locate/cej

Adsorption of copper on amine-functionalized SBA-15 prepared by co-condensation: Equilibrium properties

Enshirah Da'na, Abdelhamid Sayari*

Department of Chemical and Biological Engineering and Department of Chemistry, University of Ottawa, Ottawa, Ontario K1N 6N5, Canada

ARTICLE INFO

Article history:
Received 3 September 2010
Received in revised form 4 November 2010
Accepted 4 November 2010

Keywords:
Heavy metals removal
Mesoporous silica
Amine-functionalized SBA-15
Adsorption
Co-condensation

ABSTRACT

SBA-15 functionalized with 3-aminopropyltrimethoxy-silane was synthesized by co-condensation and used as adsorbent for Cu^{2+} ions in aqueous solution. The adsorption capacity increased dramatically with increasing temperature, initial copper concentration and pH (up to ca. 6.5). Under suitable conditions, the material exhibited high adsorption capacity even at very low copper concentration. Qualitative estimates of the thermodynamic parameters showed that the overall adsorption process is spontaneous ($\Delta G^\circ < 0$) and endothermic ($\Delta H^\circ > 0$). The adsorption isotherms of Cu^{2+} on propylamine-functionalized SBA-15 silica were best fitted by the Sips and Redlich–Peterson models. Regeneration of the adsorbent was investigated by treatment of the copper-loaded material with aqueous solution of 0.1 M HCl then 0.1 M $NaHCO_3$ or by 0.1 M EDTA solution. The adsorption uptake after ten cycles was 90% and 60% of the fresh material adsorption capacity for regeneration with EDTA and acid/base treatment, respectively.

1. Introduction

Because of the widespread presence of copper in industrial applications, e.g. electrical, electro-plating, metal finishing and paint industries, residual metal is often found in wastewater. Owing to the toxicity of copper, the World Health Organization (WHO) recommended the maximum acceptable concentration of this element in drinking water to be 2.0 mg L^{-1} [1]. Metal separation via adsorption is a very promising technique because of its simplicity and reversibility. Therefore, extensive research effort has been directed towards the development of new adsorbents for the removal of heavy metals from wastewater.

Periodic mesoporous materials exhibit many attractive characteristics such as large BET surface area, high porosity, controllable and narrowly distributed pore sizes, and often an ordered pore arrangement [2]. Thus, the development of functionalized mesoporous adsorbents for heavy metal ions using incorporated ligands with appropriate functional groups has generated considerable interest [3]. SBA-15 is among the most popular mesoporous silicas because of its large, adjustable pores (5–30 nm), which allow easier accessibility of target species to the inner surface of the material, leading to fast kinetics of chemical or physical processes, and also because of its thick pore walls, around 4 nm, which provide enhanced mechanical stability.

Two different routes were reported in the literature for the synthesis of amine-functionalized materials, namely co-condensation of the desired aminosilane with the silica precursor such as tetraethylorthosilicate (TEOS) [4–8], and post-synthesis grafting of the desired aminosilane onto the silica surface [9–16]. Compared to post-synthesis procedures, the direct co-condensation pathway often offers a better control of the resultant materials in terms of higher and more uniform surface coverage of the organic functionalities without the possible blockage of the mesopores [17–19]. In addition, co-condensation is preferred because of its simplicity and lower consumption of organic precursor. However, despite the advantages of SBA-15 as support and for co-condensation as a preparation route, amine-modified SBA-15 prepared by this method was found to have poor copper adsorption performance [20]. Since such material is synthesized in strong acidic medium, this leads to the protonation of amine, thus to the lack of adsorption capacity [21]. It was also reported that some of the amine groups might be H-bonded to neighboring surface hydroxyl groups, further diminishing their availability for adsorption [22].

To achieve the best performance for a copper ions adsorbent, a set of conditions must be met including the following (i) the occurrence of an open pore structure and accessible adsorption sites, e.g. large pore diameter; (ii) the adsorbent must be structurally stable under adsorption and regeneration conditions, e.g. treatment with acidic or basic solutions should not cause any structural damage; (iii) good contact between the copper ions and the adsorption sites, e.g. enhance the mobility of the ions within the pores and reduce the repulsion between the positive copper ions and the adsorbent surface by supplying enough energy to overcome these forces or by

* Corresponding author.
E-mail address: abdel.sayari@uottawa.ca (A. Sayari).

1385-8947/$ – see front matter © 2010 Elsevier B.V. All rights reserved.
doi:10.1016/j.cej.2010.11.016

working under suitable pH conditions to avoid a positively charged adsorbent surface. The performance of an adsorbent is related to (i) its characteristics (e.g. density and distribution of adsorption sites, structural properties), (ii) the properties of the adsorbate (e.g. concentration, size, charge, structure), and (iii) the solution conditions (e.g. pH, temperature, ionic strength). Thus, the objectives of this work were (i) to determine the thermodynamic and the equilibrium properties of copper adsorption on amine-functionalized SBA-15 prepared by co-condensation, (ii) to investigate the effect of the experimental parameters such as temperature, concentration and pH on the adsorptive properties, and (iii) to compare the regeneration and recycling of adsorbent using acid/base treatment or EDTA complexation.

2. Materials and methods

2.1. Chemicals

Tetraethylorthosilicate (TEOS) used as the silica source for SBA-15 was supplied by Aldrich. Triblock poly(ethylene oxide)-*b*-poly(propylene oxide)-*b*-poly(ethylene oxide) copolymer Pluronic P123 (MW = 5800) purchased from Aldrich was used as structure directing agent. The functionalization agent, obtained from Sigma–Aldrich was 3-aminopropyltrimethoxy-silane, herein referred to as APTS. Ultra high purity grade nitrogen and certified gas mixtures of 5% CO_2 balance N_2 were supplied by BOC Canada. All reagents and gases were used without further purification.

2.2. Adsorbent synthesis

SBA-15 was prepared according to Zhao et al. [23] with addition of KCl, for enhanced stability and ordering. The procedure was as follows: 4.0 g of P123 and 8 g KCl were dissolved in 30 mL of water and 120 mL of a 2 M HCl solution at 40 °C. Then, 8.5 g (40.8 mmol) of TEOS was added and prehydrolyzed for 2 h before adding 1.08 g (6.0 mmol) of APTS which corresponds to APTS/TEOS molar ratio of 0.15. The mixture was stirred at the same temperature for 20 h, then heated at 100 °C for 24 h in static conditions. The white solid product was collected by filtration, dried in air at room temperature for 1 day, and then extracted with ethanol (140 mL g^{-1}) at the same temperature for 24 h to remove the organic template. The material was then filtered and dried under vacuum. It will be denoted as APTS-SBA-15. To ensure complete removal of template, 1 g of the ethanol-extracted material was stirred in 50 mL of aqueous 0.1 M HCl for 1 h, filtered and dried, then neutralized in 50 mL of 0.1 M $NaHCO_3$ for 1 h and finally filtered and dried under vacuum at 100 °C for 3 h. The final material will be referred to as APTS-SBA-15-AB.

2.3. Characterization

2.3.1. Nitrogen adsorption–desorption isotherms

The structural properties of the samples before and after acid/base treatment were determined by nitrogen adsorption at 77 K using a Micromeritics ASAP 2020 volumetric apparatus. Prior to each analysis, the samples were degassed under vacuum at 60 °C for 3–5 h. The surface area was determined by the BET method, whereas the pore size distribution was calculated using the Kruk–Jaroniec–Sayari (KJS) approach [24]. The pore volume was calculated as the amount of liquid nitrogen adsorbed at $P/P_0 = 0.995$.

2.3.2. Thermal gravimetric analysis (TGA)

The amine content was determined using a thermogravimetric analyzer (Q500 TGA, TA Instruments) according to the method developed by Harlick and Sayari [25]. In the same experiment, CO_2 was used as a probe molecule to determine the accessibility of the amine functional groups within the pore channels. Briefly, the sample was first treated in a flow of ultra high purity (UHP) N_2 at 200 °C for a period of 2 h to remove preadsorbed moisture and any methanol stemming from the hydrolysis of unreacted methoxy groups. Then, it was equilibrated at 25 °C in a flow of 5% CO_2 in N_2 for 2 h. The weight gain corresponded to the CO_2 adsorption capacity. Subsequently, the organic layer was decomposed by heating at 10 °C/min to 800 °C under flowing N_2, then at 10 °C/min to 1000 °C in flowing air. The material was kept under isothermal conditions for 15 min. The amount of APTS was calculated from the weight loss, taking into consideration the CO_2 desorption, which occurs typically below 150 °C.

2.3.3. Elemental (CHN) analysis

The amine loading was also determined by elemental analysis on representative samples using a TF Flash 1112 analyzer (Thermo Finnigan). Weighed samples placed into capsules were flash-combusted at about 1800 °C and the gases were carried by helium through a reduction/oxidation column to yield N_2, CO_2 and H_2O. The gases were separated and quantified as they pass through a gas chromatograph column. The amine loading was calculated from the nitrogen content.

2.3.4. Scanning electron microscopy (SEM)

SEM was performed using a high resolution, JSM-7500F field emission scanning electron microscope from JEOL.

2.3.5. NMR measurements

^{13}C CP MAS NMR spectra were collected at room temperature on a Bruker ASX200 instrument in a magnetic field of 4.7 T (the resonance frequencies were 50.3 and 39.7 MHz, respectively).

2.3.6. Zero point charge (pH_{ZPC}) and potentiometric acid/base titrations

The surface charge properties of the APTS-SBA-15-AB were evaluated by batch equilibration technique [26]: a 100 mg sample of APTS-SBA-15-AB was introduced into a 100 mL of 0.1 M NaCl solution. The initial pH value (pH_i) of the NaCl solution was adjusted from ca. 3.0 to 11.0 by addition of 0.1 M HNO_3 or 0.1 M NaOH. The suspension was allowed to equilibrate at 20 °C for 24 h by stirring, then filtered and the pH value (pH_e) was measured again.

The surface charge properties of the APTS-SBA-15-AB were investigated by potentiometric acid/base titrations [27]: a 50 mg sample was suspended in a titration cell containing 50 mL of distilled water. The suspension was allowed to equilibrate for 24 h under continuous stirring, and then purged with N_2 for 30 min. It was subsequently divided into two portions, one each for the alkalimetric and the acidimetric titrations, using 0.1 M NaOH and 0.1 M HNO_3, respectively. In all titrations, the pH was measured with an Orion 5 stars instrument 20 min after each addition of acid or base to ensure that pH equilibrium was attained.

2.4. Preparation of copper solutions

Copper solutions were prepared by dissolving copper acetate mono-hydrate $Cu(CH_3COO)_2 \cdot H_2O$ in distilled water to obtain solutions of different concentrations. The pH of the solutions was adjusted by addition of 0.1 M HNO_3 or 0.1 M NaOH.

2.5. Equilibrium adsorption measurements and modeling

To measure the equilibrium distribution of copper ions between the adsorbent and the liquid phase, an accurately weighed amount (100 mg) of adsorbent was continuously stirred in 100 mL of copper solutions with different initial concentrations from 5 to 320 ppm.

The solution temperature was monitored using a temperature-controlled water bath. Agitation was maintained at 300 rpm for 4 h, which was verified to be sufficient to reach equilibrium. After filtration of the adsorbent, the concentration of copper in the solution was determined by inductivity coupled plasma (ICP) using a ICP-OES Varian Vista-Pro CCD spectrometer. The amount of metal adsorbed at equilibrium, q_e (mg g^{-1}), was thus calculated by:

$$q_e = \frac{(C_i - C_e)V}{W} \quad (1)$$

where C_i, C_e, V, and W are the initial and equilibrium concentrations (mg L^{-1}), volume of solution (L), and weight of adsorbent (g), respectively.

The isotherm models of Langmuir, Freundlich, Sips, and Redlich–Peterson were used to describe the equilibrium adsorption isotherms. The equations of the model isotherms are given below.

2.5.1. Langmuir isotherm

$$q_e = \frac{q_m K_L C_e}{1 + K_L C_e} \quad (2)$$

where q_m is the quantity of Cu^{2+} adsorbed at saturation or monolayer capacity (mg g^{-1}) and K_L is the Langmuir constant (L g^{-1}).

2.5.2. Freundlich isotherm

$$q_e = K_F C_e^{1/n} \quad (3)$$

where K_F is the Freundlich constant and n is the Freundlich exponent (dimensionless).

2.5.3. Sips isotherm

$$q_e = \frac{q_m K_S C_e^{1/n}}{1 + K_S C_e^{1/n}} \quad (4)$$

where q_m is the quantity of Cu^{2+} adsorbed at saturation or monolayer capacity (mg g^{-1}) and K_S (mg L^{-1})$^{-1/n}$ is the Sips constant.

2.5.4. Redlich–Peterson isotherm

$$q_e = \frac{K_{RP} C_e}{1 + a_{RP} C_e^{\beta}} \quad (5)$$

where K_{RP} (L g^{-1}) and a_{RP} (mg L^{-1})$^{-\beta}$ are the Redlich–Peterson constants and β is the Redlich–Peterson exponent (dimensionless).

The Langmuir, Freundlich, Sips, and Redlich–Peterson isotherms were used to fit the experimental data employing the linear fitting. In addition, the models were evaluated using the relative error function, which represents the summation of the squared differences of Cu^{2+} ions uptake by the adsorbent predicted by the models and the actual quantity adsorbed, q_e, measured experimentally.

The linear region of the isotherms (see Section 3.5) was used to calculate the equilibrium constant (K_c) at 293, 313 and 333 K from the slope of q_e vs. C_e. Qualitative estimation of the thermodynamic properties of the adsorption process such as enthalpy change (ΔH°), entropy change (ΔS°) and Gibbs free energy change (ΔG°) was carried out using the following equations [28]:

$$\Delta G^\circ = -RT \ln K_c \quad (6)$$

$$\ln K_c = \frac{\Delta S^\circ}{R} - \frac{\Delta H^\circ}{RT} \quad (7)$$

where R is the ideal gas constant (8.314 J K^{-1} mol^{-1}), and T is the temperature in Kelvin. ΔH° and ΔS° were obtained from the slope and intercept of Van't Hoff plot of $\ln K_c$ vs. $1/T$.

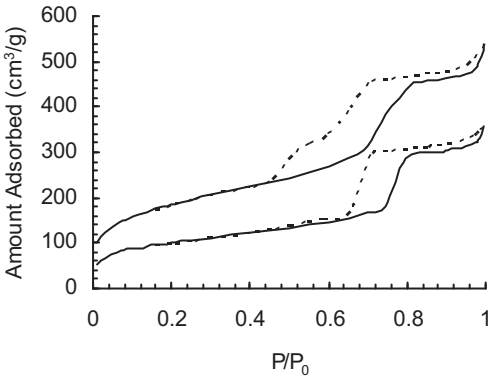

Fig. 1. Nitrogen adsorption (solid line)–desorption (dashed line) isotherms for APTS-SBA-15-AB (upper) and APTS-SBA-15 (lower).

2.6. Effect of pH

The solution pH may affect the surface charge of the adsorbents through protonation of the functional groups [21], protonation of the free surface hydroxyl groups [27], as well as the degree of ionization and hydrolysis of the species present in solution. To investigate the effect of pH, a set of experiments were performed at 293 K and several pH values between 4.0 and 6.7.

2.7. Regeneration of the adsorbent

The regeneration of the adsorbent was performed by two methods: (1) stirring the copper-loaded material in an aqueous solution of 0.1 M HCl for 1 h then neutralizing by stirring for 1 h in 0.1 M $NaHCO_3$ aqueous solution. The material was washed with distilled water and dried under vacuum at 373 K for 2 h; (2) treating the copper-loaded material with an aqueous 0.1 M sodium ethylenediaminetetraacetic acid (EDTA) solution by stirring at 333 K for 1 h, followed by washing with distilled water and drying under vacuum at 373 K for 2 h. In both methods, the solid was used for ten successive adsorption–regeneration cycles.

3. Results and discussion

3.1. Material characterization

The nitrogen adsorption–desorption isotherms of APTS-SBA-15 and APTS-SBA-15-AB are presented in Fig. 1. Both samples exhibited Type IV isotherms implying that the mesostructure is highly stable under acid/base treatment. The main structural characteristics determined experimentally are listed in Table 1. The APTS-SBA-15 exhibited pores averaging 7.9 nm in diameter, and a pore volume and surface area of 0.5 cm^3 g^{-1} and 350 m^2 g^{-1}, respectively. After the first acid/base treatment, although the mean pore size was almost the same (7.6 nm), the adsorbent exhibited significantly larger surface area (673 m^2 g^{-1}) and pore volume

Table 1
Structural properties of APTS-SBA-15 and APTS-SBA-15-AB.

	Sample	
	APTS-SBA-15	APTS-SBA-15-AB
Surface area (m^2/g)	350	673
Pore size (nm)	7.9	7.6
Pore volume (cm^3/g)	0.50	0.75
TGA amine content (mmol g^{-1})	4.4	1.75
CHN amine content (mmol g^{-1})	1.2	1.77
CO_2 adsorbed (mmol g^{-1})	0.14	0.44
Cu^{2+} adsorbed (mmol g^{-1})	0.05	0.21

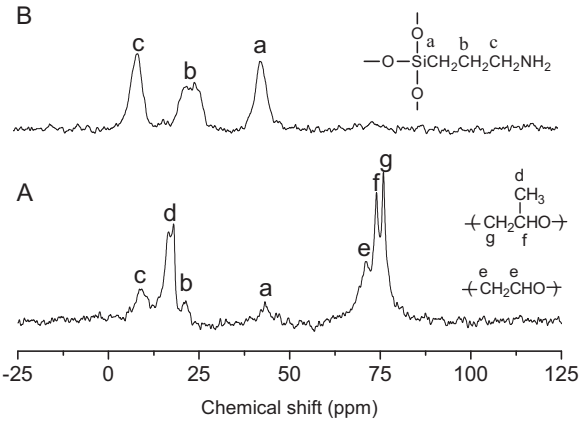

Fig. 2. ^{13}C CP MAS NMR spectra of APTS-SBA-15 after ethanol-extracted (A), and after acid/base treatment (B).

($0.75\ cm^3\ g^{-1}$). This increase in surface area and pore volume is most likely associated with the removal of residual P123 block copolymer inside the pores as corroborated by the TGA results (Table 1). Furthermore, ^{13}C MAS NMR data provided direct evidence for the occurrence of P123 in ethanol-extracted APTS-SBA-15. Fig. 2A shows that this sample exhibits NMR signals at 18.0, 71.0, 74.0 and 75.9 ppm attributable to P123; whereas the sample that underwent acid/base treatment (Fig. 2B) showed only the three signals at 9.1, 21.4 and 43.2 associated with the surface-bound propylamine.

Table 1 shows the amine content obtained by CHN elemental analysis and by TGA, CO_2 adsorption capacity obtained by TGA and copper adsorption capacity determined by ICP. The large difference in amine content obtained by the two methods for the ethanol-extracted APTS-SBA-15 sample indicates that the TGA-based value is overestimated. Indeed, the weight loss obtained by TGA of the ethanol-extracted sample did not correspond to only the decomposition of propylamine chains, but also to residual P123 polymer. Upon acid/base treatment, both amine content measurements were comparable, and the CO_2 and Cu^{2+} adsorption capacities increased significantly (Table 1). This is consistent with the complete removal of residual P123 by the acid treatment accompanied by amine protonation (Eq. (8)), and to the regeneration of the amine groups by sodium bicarbonate according to Eq. (9). Furthermore, CHN elemental analysis showed that the amine content increased after acid/base treatment, this is mainly because it was calculated on the basis of the overall material, including the residual P123, if any. The CO_2/N ratio was calculated from the CO_2 adsorption capacity obtained by TGA and compared with the stoichiometric value of 0.5, corresponding to the formation of carbamate [29]. The percentage of amine groups available for adsorption increased from 24% to 52% after acid/base treatment of the sample. The enhanced CO_2 and Cu adsorption capacity is associated with the increased accessibility of the amine groups. These results are consistent with the conclusions obtained from the nitrogen adsorption data discussed earlier. Aguado et al. [20] observed no copper adsorption using APTS-SBA-15 as prepared by co-condensation in spite of their significant nitrogen content and good structural and textural properties. This was most likely associated with the fact that the amine groups protonate under the acidic conditions of the material synthesis [21].

$$-NH_2 + H^+ \rightarrow -NH_3^+ \quad (8)$$

$$-NH_3^+ + HCO_3^- \rightarrow -NH_2 + \text{“}H_2CO_3\text{”} \quad (9)$$

Typical SEM images with different magnifications for APTS-SBA-15-AB are shown in Fig. 3. Fig. 3(a) reveals that the morphology of

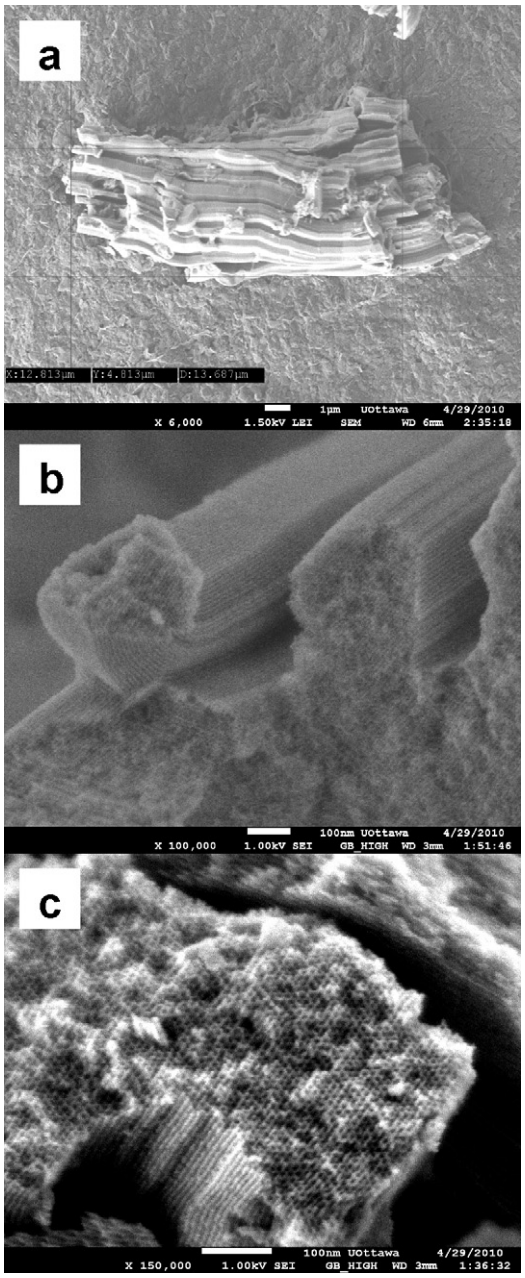

Fig. 3. SEM images of APTS-SBA-15-AB with different magnifications; bar of 1 μm for (a), and 100 nm for (b) and (c).

APTS-SBA-15-AB consists of rod-shaped particles aggregated into bundles approximately 20 μm in length and 1 μm in diameter. Higher magnification (Fig. 3(b)) shows that the particles are multifaceted and the pore channels run parallel to the particle main axis. Fig. 3(c) shows that APTS-SBA-15-AB exhibits a highly ordered hexagonal pore system, confirming the high stability of APTS-SBA-15 under acid/base treatment.

Since the surface charge of APTS-SBA-15-AB is a result of the protonation or deprotonation of surface hydroxyl as well as amine groups, one of the expected consequences of the pH_{ZPC}, which is the pH value of the solution corresponding to a net surface charge of zero (Scheme 1-1), is the dependence of adsorption of copper on the solution pH. Fig. 4 shows the equilibrium pH_e vs. the initial pH_i obtained by the batch equilibration technique for a solid to solution ratio of 1 g/L. It is evident that APTS-SBA-15-AB acts as a buffer in a wide range of pH from ca. 4 to 10. This means that for all

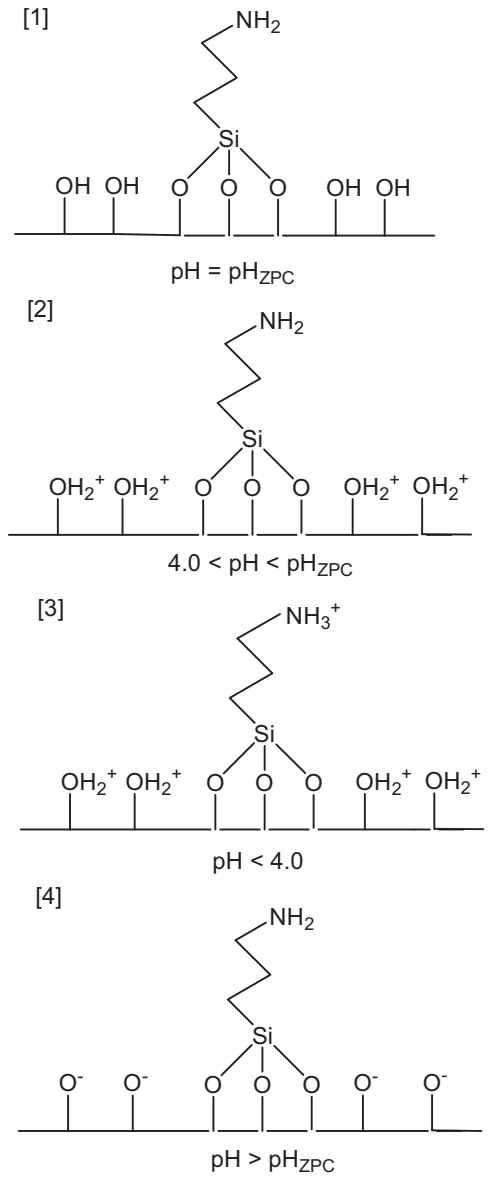

Scheme 1. Proposed surface of APTS-SBA-15-AB under different pH conditions.

values of pH_i in this range, the pH_e is the same and equal to pH_{ZPC}, which was found to be 8.62. This value is very high and implies that in aqueous solution, as the pH decreases below 8.62, the $\equiv SiOH_2^+$ species will dominate and the APTS-SBA-15-AB surface will bear a progressively increasing positive charge (Scheme 1-2). The direct implication of the high pH_{ZPC} value is that the material is not an effective copper adsorbent in a wide range of pH as it bears positive charge at pH < 8.62 considering that for copper adsorption the pH value must be kept below 6.5 to avoid precipitation of copper hydroxide (*vide infra*).

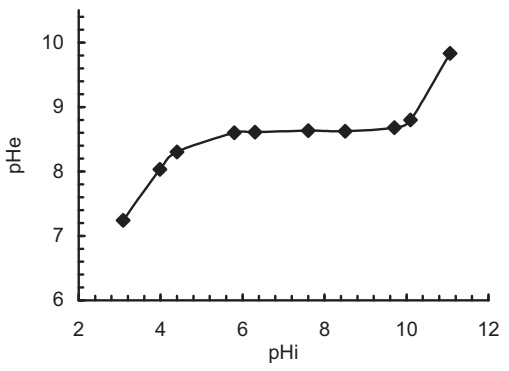

Fig. 4. pH_e as a function of pH_i for solid to solution ratio of 1 g/L, time of equilibration 24 h and background electrolyte 0.1 M NaCl.

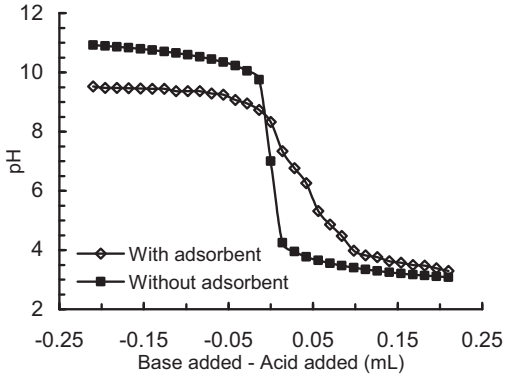

Fig. 5. Potentiometric acid/base titration.

Fig. 5 shows the acid/base potentiometric titration data with adsorbent in the solution, and the theoretical pH values calculated for a solution without the adsorbent. The horizontal axis represents the amount of acid or base added to the solutions used for the acidimetric and alkalimetric titrations, respectively. The pH_{ZPC} can be obtained from the graph at the point of zero acid or base addition to the solution containing the adsorbent, which is very close to the value obtained by batch equilibrium method (8.33 vs. 8.62). In the pH region of 4–8, any acid addition is accompanied by a significant decrease in the pH value. However, the values obtained in the presence of adsorbent are higher than the ones calculated without adsorbent, which is mainly due to the consumption of protons for the protonation of $\equiv SiOH$ sites to $\equiv SiOH_2^+$ in the region below pH_{ZPC} according to Eq. (10) (Scheme 1-2). In the pH region 3–4, the pH decreases too slowly as increasing amounts of acid are added, but always higher than the theoretical values indicating that the protons are readily consumed by the surface via amine protonation (Scheme 1-3) as the propylamine has a pK_b of 3.46 [30]. After addition of 0.2 mL of the acidic solution, the measured pH (3.3) was very close to the calculated value (3.1), indicating that most of the amine groups are protonated. At pH > 8.33, addition of base is accompanied by limited increase in the pH and the pH in this range is lower than the theoretical values due to the consumption of OH^- by the deprotonation of $\equiv SiOH$ to $\equiv SiO^-$ according to Eq. (11) (Scheme 1-4). Although at pH > 8.33, the surface of the amine-modified SBA-15 is dominated by negatively charged $\equiv SiO^-$ species, this pH region is not suitable for copper adsorption, due to the precipitation of copper hydroxide.

$$\equiv SiOH + H^+ + \leftrightarrow \equiv SiOH_2 \quad (10)$$

$$\equiv SiOH \leftrightarrow \equiv SiO^- + H^+ \quad (11)$$

3.2. Effect of temperature and initial concentration of metal ions

Solutions of different initial Cu^{2+} concentrations were used to investigate the effect of concentration on the removal of Cu^{2+}. The adsorption yield was calculated using Eq. (12):

$$\text{Removal efficiency}\,(R\%) = \left[\frac{C_i - C_e}{C_i}\right] \times 100 \quad (12)$$

As seen in Fig. 6, the removal efficiency ($R\%$) decreases by increasing the initial Cu^{2+} concentration due to saturation of binding sites, which are the limiting factor, while the Cu/N

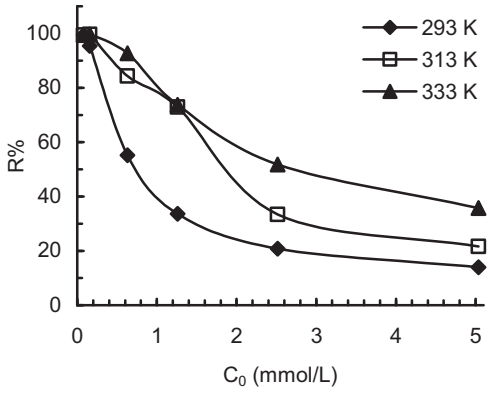

Fig. 6. Effect of temperature and initial concentration on *R*%.

atomic ratio increased as shown in Fig. 7. Kudryavtsev et al. [31] showed that at the beginning of the copper adsorption process on aminopropyl-modified silica, the ions tie with two ligands to form $[Cu(RNH_2)_2]^{2+}$complexes as shown in Scheme 2-1. Then, at higher Cu^{2+} concentration, some of the $[Cu(RNH_2)_2]^{2+}$ complexes convert into $[Cu(RNH_2)]^{2+}$ (Scheme 2-2), leading to higher adsorption capacity and higher Cu/N ratio (Fig. 7). At low concentrations, all Cu^{2+} ions present in solution could interact with two binding sites, leading to higher adsorption yield, and lower Cu/N ratio. Experiments using very dilute solutions, i.e. 5 ppm, copper was removed completely, confirming the high sensitivity of the adsorbent to such cations, which is a crucial parameter to design a copper separation process based on adsorption.

It is clear from Figs. 6 and 7 that temperature has a pronounced effect on the adsorption capacity of the adsorbent and that the effect of temperature increases as the initial copper concentration increases. The enhancement of copper uptake with increasing temperature may be attributed to the larger number of surface sites available for adsorption. As mentioned earlier, some of the amine groups might be hydrogen-bonded to the silica surface hydroxyl groups as shown in Scheme 2-3, diminishing their availability for adsorption [22]. Increasing temperature provides enough energy to break these bonds and release the amine groups (Scheme 2-4), leading to higher adsorption capacity [32]. Another possible reason is the ion-exchange reaction of Cu^{2+} with the surface hydroxyl groups via Si–O–Cu–O–Si bridging species as shown in Scheme 2-5. This was confirmed qualitatively by stirring unmodified SBA-15 silica in copper solutions at 293 and 333 K. A change in the material color into blue was observed at 333 K and the pH decreased from 6.12 to 5.09 as a result of ion-exchange between H^+ and Cu^{2+}, while the pH change at 293 K was from 6.12 to 5.88 with no change in the material color, indicating that less copper adsorption, if any was achieved. It is also possible that copper might react with one amine group and ion-exchange with an adjacent hydroxyl group as shown in Scheme 2-6. In addition, an increase in temperature provides energy to overcome repulsion forces between copper cations and the positively charged surface (Scheme 1-2), leading to higher rate of collisions between copper ions and the adsorption sites, hence, enhanced adsorption capacity.

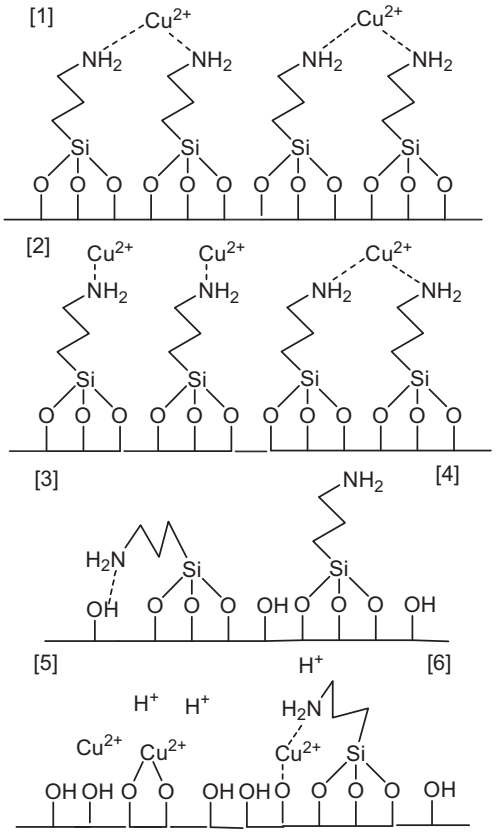

Scheme 2. Proposed mechanisms for copper adsorption on APTS-SBA-15-AB.

3.3. Thermodynamic properties

Qualitative estimates of ΔH° and ΔS° can be obtained from the slope and intercept of Van't Hoff plot $\ln K_c$ vs. $1/T$ as shown in Fig. 8. The positive value of ΔH° (47.7 kJ mol^{-1}) as shown in Table 2 indicates the endothermic nature of the overall adsorption process. This is consistent with the increase in the adsorption

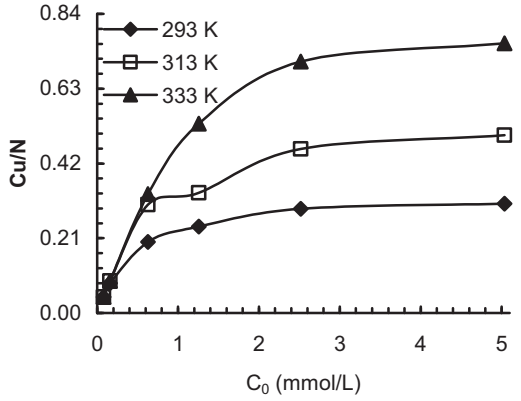

Fig. 7. Effect of temperature and initial concentration on the Cu/N ratio.

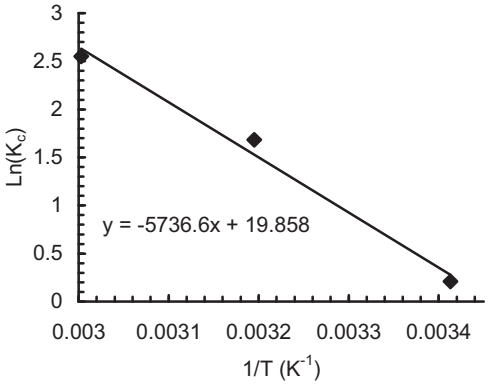

Fig. 8. Van't Hoff plot for copper adsorption on APTS-SBA-15-AB.

Table 2
Thermodynamic properties of copper adsorption on APTS-SBA-15-AB.

Temperature (K)	K_c (L g^{-1})	ΔG° (kJ mol^{-1})	ΔH° (kJ mol^{-1})	ΔS° (kJ mol^{-1})
293	1.23	−0.51	47.69	0.16
313	5.38	−4.38		
333	12.81	−7.06		

of Cu^{2+} with temperature. Endothermic adsorption of copper ions has been reported to occur on chemically modified chitosan [28], natural bentonite [33], and bentonite–polyacrylamide composites [34], while negative enthalpies have been obtained using 3-glycidoxypropyltrimethyl siloxane and propane-1,3-diamine immobilized on silica gel [35] and modified chrysotile fibers [36]. The formation of amine–copper complex being an exothermic reaction [37], it is inferred that the observed endothermic behavior is not related only to the Cu^{2+} complexation event. Since the adsorbent is highly porous and the adsorption sites are mostly located inside the pores, the endothermic behavior observed is likely to be associated with a number of endothermic processes such as diffusion resistance. In addition, the adsorption process was carried out at a pH of 6–6.5 under which the adsorbent surface is bearing a positive charge (Scheme 1-2) leading to additional energy consumption to overcome repulsive forces between the positively charged surface and the cations. Furthermore, energy is required to release the amine groups that might be hydrogen-bonded to free surface hydroxyl groups as shown in Scheme 2-3. All these processes are associated with positive enthalpies, the sum of which is larger than the negative enthalpy of formation of the amine–copper complex, leading to an overall positive enthalpy. The spontaneity of the system is expressed by the negative Gibbs free energy. Furthermore, the values of ΔG° increased with increasing temperature, indicating that the adsorption of Cu^{2+} on this adsorbent is more favorable at higher temperature. The positive entropic value is consistent with the fact that the adsorption is favorable. In fact, the positive entropic value is counterbalanced by an unfavorable endothermic enthalpy value. The positive value, which is normally associated with the displacement of the solvent initially bonded either in the cation coordination sphere or through hydrogen bonds to the amine groups [8,35]. During the adsorption process, water molecules are displaced to the medium, to cause a degree of disorder to the system and, consequently, an increase in entropy [8,35]. Positive entropy was also reported for copper removal from aqueous solutions over thiourea immobilized onto silica [35], native and modified chrysotile fibers [37], and mesoporous silica functionalized with diethylenetriamine [8].

3.4. Effect of initial pH on the adsorption of Cu^{2+}

The effect of the solution pH on the adsorption performance is shown in Fig. 9. The Cu^{2+} adsorption capacity increased gradually as the solution pH increased from 4 to 6, followed by a sharp increase at pH up to 6.5. At pH 4, the Cu/N ratio was zero and only 0.013 at a pH of 4.5. Alkylamines generally have a pK_b value around 4 [30]. This means that, at such a pH, the amine groups are mostly in the protonated form (reaction (8), Scheme 1-3), with no Cu^{2+} complexation ability. Furthermore, as the pH is lowered, the surface becomes more positive, where reaction (10) takes place [27], leading to decreased interaction between copper and the binding sites due to stronger repulsive forces which inhibit the approach of positively charged copper cations to the adsorbent surface (Scheme 1-2 and -3). Moreover, as the pH of the solution increases from 4 to 6.5, not only amine protonation according to Eq. (8) (Scheme 1) decreases, but also columbic repulsion between the surface and copper cations decreases as a result of decreasing the extent of reaction (10) [27]. Consequently, the extent of formation of coordination complex between Cu^{2+} ions and the amine groups increases, leading to higher adsorption capacity and Cu/N ratio. It is also possible that OH^- indirectly react with the weakly acidic silanol groups and breaks the hydrogen bond with the aminopropyl groups (Scheme 2-3), liberating it for adsorption. Fig. 9 shows that under otherwise the same conditions, the maximum Cu^{2+} adsorption capacity (0.6 mmol g^{-1}) was achieved at a pH of 6.5 with a Cu/N molar ratio of 0.34. When the pH increased to 6.7, precipitation of the metal hydroxide took place, accompanied by a sudden decrease in pH. It is thus inferred that the optimum pH for the removal of Cu^{2+} from aqueous solution at 293 K is 6.5. At this pH and initial concentration, neither precipitation of the metal hydroxide nor protonation of the amine groups occurs. It is worth mentioning that this optimum pH is only valid for a set of experimental conditions, i.e. temperature and concentration since precipitation depends on these parameters.

3.5. Adsorption isotherms

The adsorption isotherms of Cu^{2+} at three different temperatures 293, 313, and 333 K are shown in Fig. 10. Two-parameter models (Langmuir and Freundlich) and three-parameters models (Sips and Redlich–Peterson) isotherms were used to describe the equilibrium between Cu^{2+} and APTS-SBA-15-AB. The obtained parameters for all the models used are listed in Table 3. All the isotherms (Fig. 10) show a sharp initial slope indicating high efficiency of the material at low concentration. Furthermore, the adsorption isotherms and the calculated K_F and q_m values (Table 3) clearly show that the adsorption capacity increased with increasing temperature from 293 to 333 K, consistent with an overall endothermic process.

The isotherms constants and corresponding correlation coefficients at the three different temperatures are presented in Table 3. The three-parameter models yielded R^2 values of about 0.99, higher than the two-parameter models (R^2 values of about 0.95–0.98) demonstrating that Sips and Redlich–Peterson models more adequately fitted the data for Cu adsorption as shown in Fig. 10. Table 3 shows that the for Sips model both q_s and K_s increased linearly with increasing temperature, while n decreased linearly. For Redlich–Peterson model, both K_{RP} and a_{RP} decreased exponentially with temperature while B increased linearly. The values of n

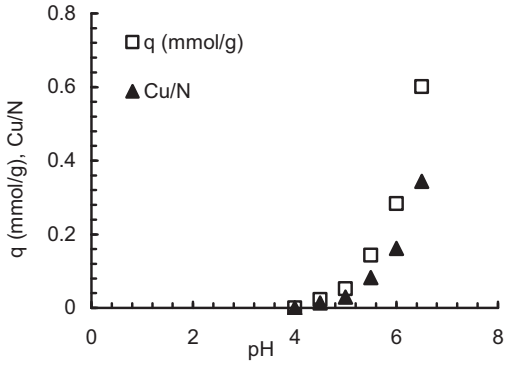

Fig. 9. Effect of initial pH on the adsorption of Cu^{2+} on APTS-SBA-15-AB.

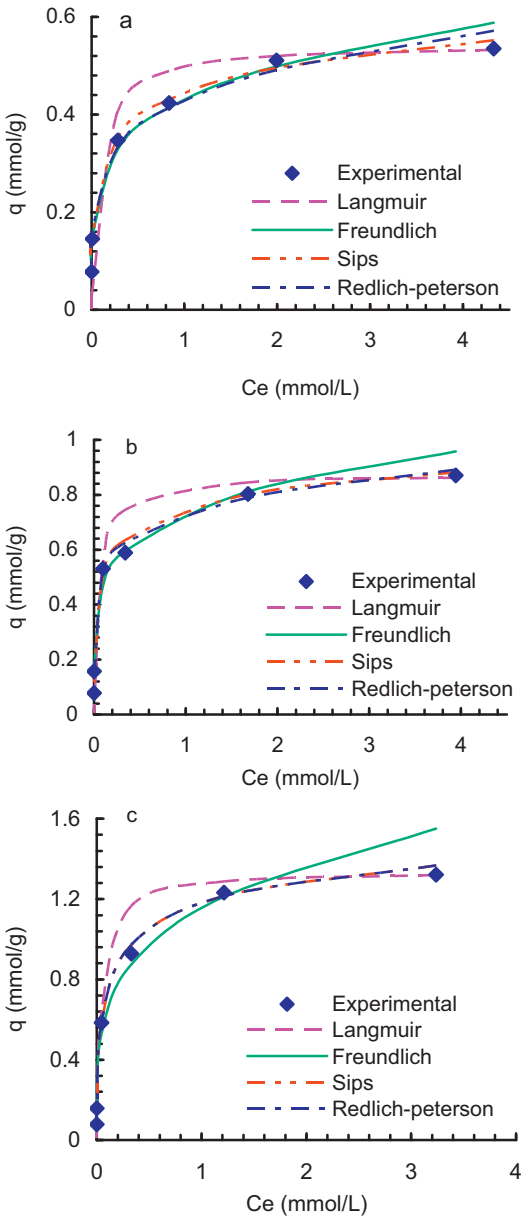

Fig. 10. Adsorption isotherms for copper on APTS-SBA-15-AB at 293 K (a), 313 K (b), and 333 K (c). Symbols show experimental values, and lines represent the calculated isotherms using Langmuir, Freundlich, Sips and Redlich–Peterson models.

in Freundlich isotherm are in the range 3.98–5.14, which indicates favorable adsorption process [33].

The maximum adsorption capacity of APTS-SBA-15-AB at 293, 313, and 333 K was found to be 0.54, 0.87 and 1.32 mmol g^{-1}, respectively, corresponding to Cu/N molar ratios of 0.31, 0.50 and 0.76. These results suggest that at 293 K, not all the amine groups were effectively used for adsorption, whereas at 333 K, the Cu/N mole ratio exceeded 0.5, which can be explained based on the effect of temperature and initial concentration as discussed earlier. Manu et al. [32] found the Cu/N mole ratio to be around 0.5 and 1 for two amine-modified silica gel samples with different loadings. They concluded that the surface density of amine groups determines the Cu/N ratio at saturation of Cu^{2+}. For comparison, the results obtained by Aguado et al. [20], at 298 K using three different samples of APTS-modified SBA-15 prepared by grafting were 0.39, 0.35, and 0.25 mmol g^{-1} with Cu/N mole ratio of 0.14, 0.11, and 0.13, respectively.

Table 3
Model parameters for adsorption of copper on APTS-SBA-15-AB.

Isotherm model	293 K	313 K	333 K
Langmuir			
q_m (mmol g^{-1})	0.54	0.88	1.34
K_L (L g^{-1})	10.62	17.10	20.34
R^2	0.959	0.958	0.969
Function error, F_{error}	0.025	0.054	0.089
Freundlich			
K_F	0.43	0.73	1.15
N	4.70	5.14	3.98
R^2	0.983	0.970	0.964
Function error, F_{error}	0.003	0.019	0.067
Sips			
q_s (mmol g^{-1})	0.93	1.24	1.74
K_s	0.91	1.53	2.01
N	3.16	2.87	2.22
R^2	0.997	0.989	0.990
Function error, F_{error}	0.001	0.006	0.007
Redlich–Peterson			
K_{RP} (L g^{-1})	8613	932	781
a_{RP}	17613	1162	600
B	0.759	0.741	0.731
R^2	0.987	0.991	0.996
Function error, F_{error}	0.002	0.005	0.016

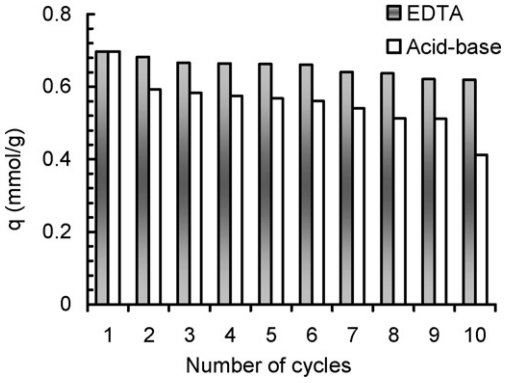

Fig. 11. Adsorption capacity of regenerated adsorbent for 10 cycles.

3.6. Regeneration of the adsorbent

In addition to excellent adsorption capacity, it is highly desirable that an adsorbent can be regenerated and reused repeatedly, for improved process economics. Fig. 11 shows that recycling using EDTA regeneration was more efficient than acid/base treatment. The adsorption capacity after ten cycles was 90% in comparison to the fresh material, while for acid/base treatment, the adsorption capacity after ten cycles was only 60% of the initial capacity. However, for both regeneration methods, the actual loss of amine after ten cycles was less than 10%, indicating that in the case of acid/base regeneration, not all the amine groups were recovered possibly due to incomplete release of copper after acidic treatment. This is consistent with the light blue color of regenerated samples.

4. Conclusions

Adsorption of Cu^{2+} on amine-functionalized SBA-15 prepared by co-condensation followed by treatment in acidic then basic solutions was studied under different conditions. The adsorbent showed very high sensitivity and efficiency for removing copper from very dilute solutions, which is a crucial requirement for practical applications. Increasing the temperature, the copper initial concentration and pH resulted in higher adsorption capacity. The

calculated thermodynamic properties indicated the occurrence of a spontaneous and endothermic process. The adsorption data correlated well with the Sips model and Redlich–Peterson model. Regeneration of the adsorbent was evaluated by treatment of the copper-loaded materials with 0.1 M aqueous solutions of HCl then $NaHCO_3$ or by EDTA at 333 K. The adsorption capacity after ten cycles was 90% and 60% in comparison to the fresh material for regeneration with EDTA and acid/base, respectively.

Acknowledgments

The financial support of the Natural Science and Engineering Council of Canada (NSERC) is acknowledged. A.S. thanks the Federal Government for the Canada Research Chair in *Nanostructured Materials for Catalysis and Separation* (2001–2015).

References

[1] World Health Organization, Guidelines for drinking-water quality: Recommendations—Addendum, vol. 1, 3rd ed., 2008.
[2] J.S. Beck, J.C. Vartuli, W.J. Roth, M.E. Leonowicz, C.T. Kresge, K.D. Schmitt, C.T-W. Chu, D.H. Olson, E.W. Sheppard, S.B. McCullen, J.B. Higgins, J.L. Schlenker, A new family of mesoporous molecular sieves prepared with liquid crystal templates, J. Am. Chem. Soc. 114 (1992) 10834–10843.
[3] A. Sayari, S. Hamoudi, Periodic mesoporous silica-based organic–inorganic nanocomposite materials, Chem. Mater. 13 (2001) 3151–3168.
[4] L. Bois, A. Bonhommeĭ, A. Ribes, B. Pais, G. Raffin, F. Tessier, Functionalized silica for heavy metal ions adsorption, Colloids Surf. A: Physicochem. Eng. Aspects 221 (2003) 221–230.
[5] K. Inumaru, Y. Inoue, S. Kakii, T. Nakano, S. Yamanaka, Molecular selective adsorption of dilute alkylphenols and alkylanilines from water by alkyl-grafted MCM-41: tunability of the cooperative organic–inorganic function in the nanostructure, Phys. Chem. Chem. Phys. 6 (2004) 3133–3139.
[6] J. Aguado, J.M. Arsuaga, A. Arencibia, Adsorption of aqueous mercury (II) on propylthiol-functionalized mesoporous silica obtained by cocondensation, Ind. Eng. Chem. Res. 44 (2005) 3665–3671.
[7] J. Aguado, J.M. Arsuaga, A. Arencibia, Influence of synthesis conditions on mercury adsorption capacity of propylthiol functionalized SBA-15 obtained by co-condensation, Micropor. Mesopor. Mater. 109 (2008) 513–524.
[8] R.K. Dey, F.J.V.E. Oliveira, C. Airoldi, Mesoporous silica functionalized with diethylenetriamine moieties for metal removal and thermodynamics of cation-basic center interactions, Colloids Surf. A: Physicochem. Eng. Aspects 324 (2008) 41–46.
[9] O. Olkhovyk, V. Antochshuk, M. Jaroniec, Benzoythiourea-modified MCM-48 mesoporous silica for mercury (II) adsorption from aqueous solutions, Colloids Surf. A: Physicochem. Eng. Aspects 236 (2004) 69–72.
[10] Y. Shiraishi, G. Nishimura, T. Hirai, I. Komasawa, Separation of transition metals using inorganic adsorbents modified with chelating ligands, Ind. Eng. Chem. Res. 41 (2002) 5065–5070.
[11] V. Antochshuk, M. Jaroniec, 1-Allyl-3-propylthiorea modified mesoporous silica for mercury removal, Chem. Commun. (2002) 258–259.
[12] A.M. Liu, K. Hidajat, S. Kawi, D.Y. Zhao, A new class of hybrid mesoporous materials with functionalized organic monolayers for selective adsorption of heavy metal ions, Chem. Commun. (2000) 1145–1146.
[13] L. Zhang, C. Yu, W. Zhao, Z. Hua, H. Chen, L. Li, J. Shi, Preparation of multi-amine-grafted mesoporous silicas and their application to heavy metal ions adsorption, J. Non-Cryst. Solids 353 (2007) 4055–4061.
[14] X. Feng, G. Fryxell, L.Q. Wang, A.Y. Kim, J. Liu, K.M. Kemner, Functionalized monolayers on ordered mesoporous supports, Science 276 (1997) 923–926.
[15] J. Liu, X. Feng, G. Fryxell, L.-Q. Wang, A. Kim, M. Gong, Hybrid mesoporous materials with functionalized monolayers, Adv. Mater. 10 (1998) 161–165.
[16] H. Lee, J. Yi, Removal of copper ions using functionalized mesoporous silica in aqueous solution, Sep. Sci. Technol. 36 (2001) 2433–2448.
[17] T. Yokoi, H. Yoshitake, T. Tatsumi, Synthesis of amino-functionalized MCM-41 via direct co-condensation and post-synthesis grafting methods using mono-, di-, and tri-amino-organalkoxysilane, J. Mater. Chem. 14 (2004) 951–957.
[18] M. Jaroniec, K. Kruk, C. Jaroniec, A. Sayari, Modification of surface and structural properties of ordered mesoporous silicates, Adsorption 5 (1999) 39–45.
[19] X. Wang, J.C. Chan, Y.H. Tseng, S. Cheng, Synthesis, characterization and catalytic activity of ordered SBA-15 materials containing high loading of diamine functional groups, Micropor. Mesopor. Mater. 95 (2006) 57–65.
[20] J. Aguado, J.M. Arsuaga, A. Arencibia, M. Lindo, V. Gascón, Aqueous heavy metals removal by adsorption on amine-functionalized mesoporous silica, J. Hazard. Mater. 163 (2009) 213–221.
[21] A.S. Chong, X.S. Zhao, Functionalization of SBA-15 with APTES and characterization of functionalized materials, J. Phys. Chem. B 107 (2003) 12650–12657.
[22] K.F. Lam, X. Chen, G. McKay, K.L. Yeung, Anion effect on Cu^{2+} adsorption on NH_2-MCM-41, Ind. Eng. Chem. Res. 47 (2008) 9376–9383.
[23] D. Zhao, Q. Huo, J. Feng, B.F. Chmelka, G.D. Stucky, Nonionic triblock and star diblock copolymer and oligomeric surfactant syntheses of highly ordered, hydrothermally stable, mesoporous silica structures, J. Am. Chem. Soc. 120 (1998) 6024–6036.
[24] M. Kruk, M. Jaroniec, A. Sayari, Application of large pore MCM-41 molecular sieves to improve pore size analysis using nitrogen adsorption measurements, Langmuir 13 (1997) 6267–6273.
[25] P. Harlick, A. Sayari, Applications of pore-expanded mesoporous silica. 3. Triamine silane grafting for enhanced CO_2 adsorption, Ind. Eng. Chem. Res. 45 (2006) 3248–3255.
[26] I.D. Smičiklas, S.K. Milonjić, P. Pfendt, S. Raičević, The point of zero charge and sorption of cadmium (II) and strontium (II) ions on synthetic hydroxyapatite, Sep. Purif. Technol. 18 (2000) 185–194.
[27] K. Dimos, P. Stathi, M.A. Karakassides, Y. Deligiannakis, Synthesis and characterization of hybrid MCM-41 materials for heavy metal adsorption, Micropor. Mesopor. Mater. 126 (2009) 65–71.
[28] B. Kannamba, K.L. Reddy, B.V. AppaRao, Removal of Cu(II) from aqueous solutions using chemically modified chitosan, J. Hazard. Mater. 175 (2010) 939–948.
[29] R. Serna-Guerrero, E. Da'na, A. Sayari, New insights into the interactions of CO_2 with amine-functionalized silica, Ind. Eng. Chem. Res. 47 (2008) 9406–9412.
[30] D.R. Lide, W.M.M. Haynes, Handbook of Chemistry and Physics, 90th ed., 2010, pp. 8–43.
[31] G.V. Kudryavtsev, D.V. Miltchenko, V.V. Yagov, A.A. Lopatkin, Ion sorption on modified silica surface, J. Colloid Interface Sci. 140 (1990) 114–122.
[32] V. Manu, H.M. Mody, H.C. Bajaj, R.V. Jasra, Adsorption of Cu^{2+} on amino functionalized silica gel with different loading, Ind. Eng. Chem. Res. 48 (2009) 8954–8960.
[33] N. Karapinar, R. Donat, Adsorption behaviour of Cu^{2+} and Cd^{2+} onto natural bentonite, Desalination 249 (2009) 123–129.
[34] G. Zhao, H. Zhang, Q. Fan, X. Ren, J. Li, Y. Chen, X. Wang, Sorption of copper(II) onto super-adsorbent of bentonite–polyacrylamide composites, J. Hazard. Mater. 173 (2010) 661–668.
[35] F.J.V.E. Oliveira, E.C. da Silva Filho, M.A. Melo, C. Airoldi, Modified coupling agents based on thiourea, immobilized onto silica. Thermodynamics of copper adsorption, Surf. Sci. 603 (2009) 2200–2206.
[36] J.A.A. Sales, C. Airoldi, Calorimetric investigation of metal ion adsorption on 3-glycidoxypropyltrimethylsiloxane + propane-1,3-diamine immobilized on silica gel, Thermochim. Acta 427 (2005) 77–83.
[37] M.G. Fonseca, C. Airoldi, Thermodynamics data of interaction of copper nitrate with native and modified chrysotile fibers in aqueous solution, J. Colloid Interface Sci. 240 (2001) 229–236.